

# The Mechanisms of Hydrogenolysis and Isomerization of Hydrocarbons on Metals. VIII. Isomerization of $^{13}\text{C}$ Labeled Pentanes on a 10% Pt- $\text{Al}_2\text{O}_3$ Catalyst

François Garin and François G. Gault\*

Contribution from the Laboratoire de Catalyse, Université Louis Pasteur de Strasbourg, Strasbourg, France. Received August 15, 1974

**Abstract:** The isomerization and hydrocracking of pentanes have been studied over a 10% Pt- $\text{Al}_2\text{O}_3$  catalyst of low dispersion at 250–300°. The use of labeled compounds, *n*-pentane-2- $^{13}\text{C}$  and 2-methylbutane-2- $^{13}\text{C}$ , allowed one to distinguish between the various parallel and consecutive reactions and to determine their apparent activation energies and orders vs. hydrogen. According to the kinetic data, the skeletal rearrangements of pentanes may be classified in four groups: I, *n*-pentane → *n*-pentane isomerization according to a cyclic mechanism; II, isopentane → *n*-pentane isomerization and the reverse reaction; III, methyl shift, isopentane → neopentane isomerization and hydrogenolysis of the internal C–C bonds; IV, demethylation. The very high negative orders vs. hydrogen found in each case suggest that the adsorbed intermediates responsible for the various reactions are formed by the succession of bimolecular elementary steps involving adsorbed hydrogen. Some suggestions are made on the nature of these intermediates.

Following the pioneer work of Kazanskii, Liberman, and Plate who showed that a number of hydrocarbon reactions, such as hydrogenolysis of cyclopentanes,<sup>1</sup> dehydrocyclization, and aromatization of substituted pentanes,<sup>2–5</sup> take place on metals, it was very soon suspected that the skeletal isomerization of hydrocarbons on supported metal catalysts could be promoted by the metal itself without the contribution from an acidic carrier proposed in the classical “bi-functional” mechanism.<sup>6</sup> Isomerization of hydrocarbons takes place indeed on platinum or palladium films and on supported platinum catalysts under conditions (200–300°) such that the support (glass or alumina) cannot be suspected of having any catalytic properties.<sup>7,8</sup>

Two reaction mechanisms were put forward in order to explain the skeletal isomerization of hydrocarbons on metals. The “bond shift mechanism” (Figure 1a) explains the

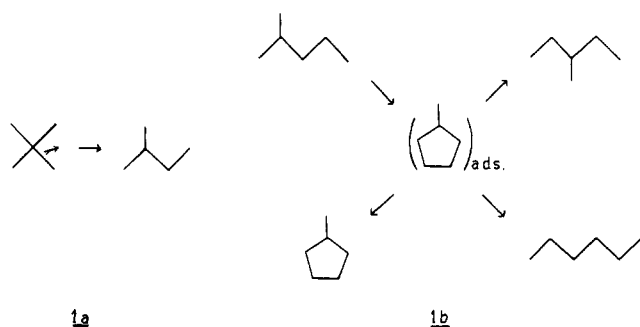


Figure 1.

isomerization of short molecules (isobutane and neopentane).<sup>9</sup> When the carbon chain is long enough and on highly dispersed catalysts (0.2% Pt- $\text{Al}_2\text{O}_3$ , for example), another mechanism takes place, which involves the dehydrocyclization to an adsorbed cyclopentane intermediate followed by rupture of the ring and desorption of the products.<sup>8</sup> Figure 1b illustrates the various elementary steps which would occur in this “cyclic mechanism” in the case of hexanes.

On most platinum catalysts, either films or supported platinum with a moderate degree of dispersion, both the cyclic and the bond shift mechanisms take place. The first problem which arises is that of determining the contribution of each. In most recent work, hexane isomerization was used as the test reaction and the amount of methylcyclopentane in the reaction products was taken as a measure of the

relative importance of the cyclic mechanism.<sup>10,11</sup> Such an estimate is rather misleading: first the rate of methylcyclopentane hydrogenolysis is much larger than the rate of isomerization, by roughly two orders of magnitudes, so that the concentration of methylcyclopentane in the reaction products is highly dependent upon the conversion, even when it is very small;<sup>8b</sup> second the ratio between ring opening and methylcyclopentane desorption depends largely upon the experimental conditions and the nature of the catalyst.

For these reasons the simple analysis of product distributions was not considered as safe enough and tracer techniques were preferred in order to estimate the contribution of either mechanism.<sup>12–14</sup> Figure 2 shows for example how

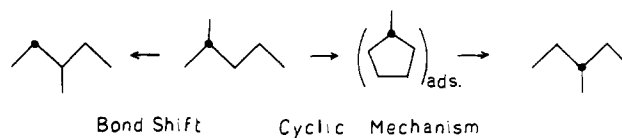
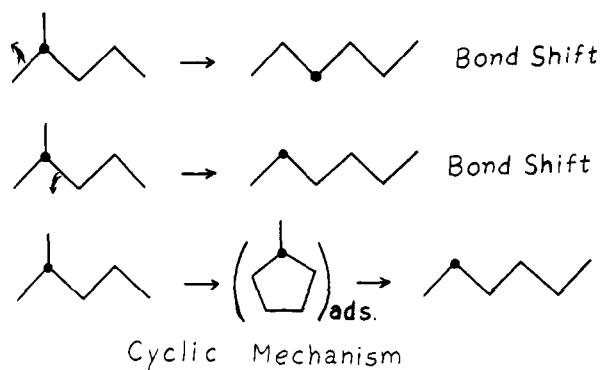


Figure 2.

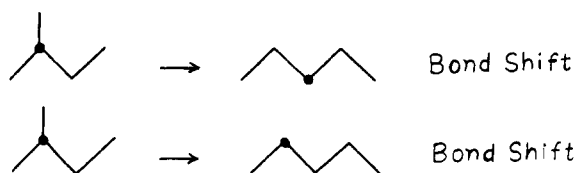
the use of 2-methylpentane-2- $^{13}\text{C}$  allows one to distinguish between the “bond shift” and the “cyclic” mechanism of isomerization.

A second problem, which arises in the field of skeletal rearrangement on metal, is the elaboration of a consistent and detailed description of the various elementary steps. This problem has not yet been solved. For the bond shift isomerization, for example, four different mechanisms have been proposed so far.<sup>15–17</sup> However, none of the arguments put forward to support any of these mechanisms seemed really convincing. In order to ascertain the reaction mechanism for bond shift and cyclic type isomerization, it seemed then desirable to combine kinetic and tracer studies. On one hand, the use of labeled hydrocarbons allows one to isolate the various elementary reactions; on the other hand the knowledge of their apparent activation energies and orders, and particularly a comparison between them, may be very useful in order to determine the detailed mechanisms.

Isomerization of pentanes labeled with  $^{13}\text{C}$  was investigated and is described in this paper. The hydrocarbons, pentanes instead of hexanes, were chosen for the sake of simplification. For example, isomerization of methyl-2-pentane to *n*-hexane occurs by three different reactions:



However, only two easily distinguishable reactions occur for the isomerization of isopentane to *n*-pentane.



### Experimental Section

**Materials. Alcohols.** Several  $^{13}\text{C}$  labeled pentanols (see Table I) were synthesized by reacting a ketone, aldehyde, or ester with an alkylmagnesium halide. The procedure to prepare these compounds in small quantities (ca. 50 mg) and with a reasonable yield, 65–70%, has already been described.<sup>12,18</sup> The isotopic purity of the starting materials, methyl ( $^{13}\text{C}$ ) iodide, ethyl- $^{13}\text{C}$  iodide, sodium formate ( $^{13}\text{C}$ ), and acetone-2- $^{13}\text{C}$ , obtained from Merck Sharpe & Dohme (Canada), was in some cases around 60% and in some cases around 90%.

**Hydrocarbons.** All the possible  $^{13}\text{C}$  labeled *n*-pentanes and isopentanes used for the catalytic experiments and the mass spectrometrical calibrations were prepared from the appropriate labeled alcohols. Dehydration over 0.8 g of alumina and hydrogenation at 120° of the resulting olefin over 1 g of 10% Pt- $\text{Al}_2\text{O}_3$  were carried out in the same pulse flow system already described.<sup>12</sup> The temperature of the alumina, 220°, was such that the extent of skeletal rearrangement and cracking, taking place during the dehydration, was less than 1%. The impurities resulting from these side reactions were removed by gas chromatography, before the labeled hydrocarbons were used in the catalytic experiments. The unlabeled hydrocarbons were Fluka puriss grade and were used without further purification.

**Catalysts.** The 10% Pt- $\text{Al}_2\text{O}_3$  catalyst was prepared by impregnation by a chloroplatinic solution of the same inert alumina (obtained from Woelm A.G.: specific area 164  $\text{m}^2/\text{g}$ ; mean pore diameter 34 Å; no metal detected by X-ray fluorescence; sulfur content 30 ppm), which has been used in previous studies.<sup>12–14</sup> The reduction was performed at 100° with a hydrogen flow rate of 10 ml/min and completed at 200° during 48 hr. Hydrogen chemisorption, oxygen-hydrogen titration<sup>19</sup> and X-ray line broadening measurements gave the same value of 90 Å for the mean metal crystallite diameter. The same alumina and the same platinum/alumina were used as dehydration and hydrogenation catalysts during the preparation of the labeled hydrocarbons.

**Apparatus and Procedure.** The catalytic reactions were carried out in an all-glass, grease-free flow system already described.<sup>20</sup> The catalyst bed (ca. 200 mg) was isothermal and isobaric and operated under differential conditions. A small amount of reactant (ca. 4 mg) was used for each run and injected into the reactor at constant pressure (2 to 10 Torr). A katharometer, inserted in the flow line between the injection device and the reactor, enabled the recording of the pressure vs. time curve, which approximated closely to a square-wave pulse. From this curve, after calibration, it was possible to deduce the hydrocarbon pressure and the hydrocarbon flow rate.

Samples for gas chromatographic analysis were removed directly from the gas phase by a gas syringe as the pulse passed a rubber

Table I. Synthesis of Labeled Alcohols

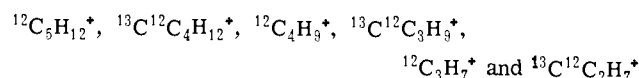
Carbon skeleton	RC(=O)R'	R''MgX	RR'R''COH
	Acetone-2- $^{13}\text{C}$	BrMgEt	2-Methyl-2-butanol-2- $^{13}\text{C}$
	2-Butanone	IMg $^{13}\text{CH}_3$	Methyl( $^{13}\text{C}$ )-2-butanol
	Acetone	IMg $^{13}\text{CH}_2\text{-CH}_3$	2-Methyl-2-butanol-3- $^{13}\text{C}$
	2-Methylpropanal	IMg $^{13}\text{CH}_3$	3-Methyl-2-butanol-1- $^{13}\text{C}$
	Butanal	IMg $^{13}\text{CH}_3$	2-Pentanol-1- $^{13}\text{C}$
	Propanal	IMg $^{13}\text{CH}_2\text{CH}_3$	3-Pentanol-2- $^{13}\text{C}$
	Ethyl formate ( $^{13}\text{C}$ )	2BrMgEt	3-Pentanol-3- $^{13}\text{C}$

septum located close to the reactor. Most of the hydrocarbons issuing from the reactor were collected in a trap during the plateau of the  $P = f(t)$  curve, which lasted several minutes. The various molecules were then separated by gas chromatography and their mass spectra recorded.

**Gas Chromatography.** GLC analyses were performed on a 5 m  $\times$   $\frac{1}{8}$  in. Silicone-DC-200/firebrick column operating at  $-15^\circ$ . The molar concentrations were obtained from the GLC data by using the sensitivity data of Dietz<sup>21</sup> for hydrogen flame detectors. The purification of the tracing labeled hydrocarbon and the separation of the products were carried out at 0° on a 5 m  $\times$  0.25 in. silicone SE30/firebrick column.

**Mass Spectrometry.** The mass spectrometrical analysis was performed with a CH7 Varian-Mat apparatus operating with 70 V electrons and a trap current of 300  $\mu\text{A}$ . A resolution of 1500–2000 was needed to separate the hydrocarbon fragment ions from  $\text{CO}_2^+$  and the silicone fragments (essentially  $\text{SiO-CH}_3^+$  at mass 44) which result from some silicone compounds eluted from the GLC columns during the previous operations.

The mass spectra were recorded in the parent,  $-\text{CH}_3$  and  $-\text{C}_2\text{H}_5$ , regions. The treatment of the data has already been described in detail.<sup>12,18</sup> After correction for the naturally occurring



isotopes and the C-H fragmentation, the amounts of the main ions were determined in each group of masses. From the ratios

$$\begin{aligned} r_5 &= ^{13}\text{C}^{12}\text{C}_4\text{H}_{12}^+ / ^{12}\text{C}_5\text{H}_{12}^+ \\ r_4 &= ^{13}\text{C}^{12}\text{C}_3\text{H}_9^+ / ^{12}\text{C}_4\text{H}_9^+ \\ r_3 &= ^{13}\text{C}^{12}\text{C}_2\text{H}_7^+ / ^{12}\text{C}_3\text{H}_7^+ \end{aligned}$$








are calculated the mole fractions  $a_4$  and  $a_3$  of the ions  $\text{C}_4\text{H}_9^+$  and  $\text{C}_3\text{H}_7^+$  which have retained the carbon-13 during their formation from an isotopically pure labeled hydrocarbon.

The values of  $a_4$  and  $a_3$  for all the possible labeled pentanes and isopentanes are reported in Table II. As it was already pointed out,<sup>18</sup> the fragment  $-\text{CH}_3$  in *n*-pentane corresponds either to the loss of the terminal carbon atoms  $\text{C}_1$  and  $\text{C}_5$  or of the central carbon atom  $\text{C}_3$ . The  $a_4$  and  $a_3$  values of isopentanes are close to those expected if the terminal  $\text{CH}_3$  or  $\text{C}_2\text{H}_5$  groups were eliminated during the fragmentation.

The location of the carbon-13 in the various molecules after reaction was found in general by comparing the observed values  $a_4$  and  $a_3$  with the  $a_{4i}$  and  $a_{3i}$  values of the reference hydrocarbons. In the case of the *n*-pentanes, the following set of equations allows one to calculate the concentrations  $c_i$  of the various isotopic species  $i$  in the reaction mixture, with an accuracy of ca.  $\pm 1\%$ .

$$\begin{aligned} a_4 &= \sum_i c_i a_{4i} \\ a_3 &= \sum_i c_i a_{3i} \\ 1 &= \sum_i c_i \end{aligned} \quad (\text{I})$$

Table II. Mass Spectra of Pentanes Labeled with Carbon-13 ( $a_3$  and  $a_4$  Values)<sup>a</sup>

Hydrocarbon		$a_4$	$a_3$
	I-X	0.64	0.51
	I-Y	0.995	0.51
	I-Z	0.77	0.970
	II-X	0.525	0.950
	II-Y	1.00	0.96
	II-Z	1.00	0.055
	II-T	0.95	0.080

<sup>a</sup> The possible error for the values of  $a_4$  and  $a_3$  is  $\pm 0.005$ .

In the case of the isopentanes, the values of  $a_4$  and  $a_3$  for the 2-methylbutanes 3-<sup>13</sup>C (II-Z) and 4-<sup>13</sup>C (II-T) are very close. On account of these similarities, it is possible to determine, by using a set of equations such as I to determine, with an accuracy of  $\pm 2\%$ , the concentrations of II-X, II-Y, and of the sum II-Z + II-T. When it is possible to eliminate, on chemical grounds, one of the varieties (II-T, for example), eq I may be solved exactly and the error is decreased down to  $\pm 0.5\%$ .

**Determination of the Reaction Rates.** Provided that the mole fraction  $\alpha$  of the reactant which has been converted is small enough, which is the case in most of the reactions considered, the following relationship

$$r = \alpha(F/w) \quad (1)$$

allows one to calculate the reaction rate as a function of the hydrocarbon flow rate  $F$  and the weight of catalyst  $w$ . Equation 1 holds also when several parallel reactions take place, and whatever the order vs. hydrocarbon may be.

When the conversion  $\alpha$  is high (methyl shift in isopentane), the following differential eq 2 may be derived, if one assumes that both the direct and the reverse reactions are first order vs. hydrocarbon

$$d\alpha = r(1 - \alpha) - r\alpha(dw/F) \quad (2)$$

whence

$$r = \log \frac{1}{1/2 - \alpha} \frac{F}{w}$$

## Results and Interpretation

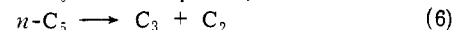
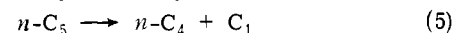
**(I) Isomerization and Hydrocracking of *n*-Pentane and Isopentane. Product Distributions.** The reactions of *n*-pentane and isopentane have been studied over 10% Pt-Al<sub>2</sub>O<sub>3</sub> at constant hydrocarbon pressure (3 and 5 Torr, respectively) and at various hydrogen pressures (300–1200 Torr) and temperatures (255–285°).

In the case of *n*-pentane, the three main reactions were: hydrocracking yielding methane, ethane, propane and *n*-butane; isomerization to isopentane, and dehydrocyclization to cyclopentane. The overall conversion was kept below 10%, so that the product distributions could be considered as being very close to the initial ones. The validity of this assumption was demonstrated by the isobutane-*n*-butane ratio, always smaller than 0.03.

In each experiment, the mole fractions of ethane and propane among the cracking products were exactly equal, and very often the mole fractions of methane and butanes. In some experiments, however, on account of a change of sensitivity of the flame ionization detector, too low a value was found for the methane concentration. (Since the products are injected in a large excess of hydrogen, the sensitivity of the flame detector may change momentarily, during the elution of the hydrogen and also of the methane, which fol-

lowed closely after.) It was assumed that in these cases also equal amounts of methane and butanes were formed. Lastly, in one experiment at low hydrogen pressure, the methane molecules widely outnumbered the butane molecules, showing that a complete degradation of *n*-pentane to methane took place.

In Table III are given, for various experimental conditions, the percentages of *n*-pentane which reacted according to reactions 3–7.



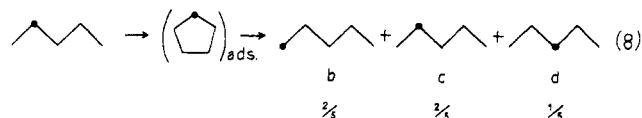
The ratio  $\rho_1$ , cracking/isomerization, and  $\rho_2$ , internal fission (eq 6)/demethylation (eq 5) are also given in the two last columns of Table III. A decrease of temperature or an increase of hydrogen pressure favors hydrogenolysis vs. isomerization and demethylation vs. internal fission.

Since hydrogenolysis of cyclopentane is much faster than isomerization and hydrocracking of alkanes, the amount of cyclopentane is highly dependent upon the conversion (see, i.e., runs 2 and 5); one may notice, however, from the table a tendency to increase the dehydrocyclization when the temperature is increased or the hydrogen pressure decreased.

**The three main reactions of isopentane over Pt-Al<sub>2</sub>O<sub>3</sub>** are demethylation (to *n*-butane or isobutane), internal fission (yielding propane and ethane), and isomerization to *n*-pentane. Isomerization to neopentane is also observed in each experiment, and a complete degradation to methane takes place in one experiment at low hydrogen pressure. The absence of cyclopentane among the reaction products shows that successive reactions are negligible, and so the product distributions may be considered as very close to the initial ones.

In Table IV are given the overall conversion  $\alpha$ , the relative contributions of the various reactions, and the ratios  $\rho_1$  (cracking/isomerization),  $\rho_2$  (internal fission/demethylation), and  $\rho_3$  (*n*-butane/isobutane).  $\rho_3$  does not depend upon temperature and increases only slightly with hydrogen pressure. As was observed previously in the case of *n*-pentane, an increase of hydrogen pressure and a decrease of temperature favors hydrocracking vs. isomerization and demethylation vs. internal fission.

**(II) Isomerization of *n*-Pentane-2-<sup>13</sup>C.** The contact reactions of *n*-pentane-2-<sup>13</sup>C on 10% Pt-Al<sub>2</sub>O<sub>3</sub> were studied under the same experimental conditions as in section I, in order to compare hydrocracking and isomerization to isopentane with the *n*-pentane  $\rightarrow$  *n*-pentane isomerization via a cyclic mechanism (reaction 8). Reaction 8 can only be ob-



served when using labeled hydrocarbons.

In Table V are given the distributions of the various isotopic varieties (of *n*-pentanes and isopentanes).

***n*-Pentanes.** Since the mole fractions  $b$  and  $d$  of *n*-pentane-1-<sup>13</sup>C and 3-<sup>13</sup>C are very small, they were determined by using<sub>2</sub> instead of the three usual linear equations 9–11, eq 9 and 10 plus eq 12, implied by the supposed isomerization mechanism 8. The sum  $S = b + c + d$  was then calcu-

Table III. Reactions of *n*-Pentane over 10% Pt–Al<sub>2</sub>O<sub>3</sub> (Product Distributions)

Run	$P_{H_2}$	$T, ^\circ C$	$\alpha, \%$	5CH <sub>4</sub>	CH <sub>4</sub> + C <sub>4</sub> H <sub>10</sub>	C <sub>2</sub> H <sub>6</sub> + C <sub>3</sub> H <sub>8</sub>	<i>i</i> -C <sub>5</sub> H <sub>12</sub>	<i>c</i> -C <sub>5</sub> H <sub>10</sub>	$\rho_1$	$\rho_2$
1	760	258	9.3	0	25.0	42.4	30.7	1.9	2.05	1.7
2	760	269	9.7	0	19.7	39.4	38.3	2.6	1.45	2.0
3	760	284	8.1	0	15.7	35.8	44.5	4.0	1.05	2.3
4	312	269	6.5	5.6	9.6	33.2	43.9	7.7	0.85	3.45
5	760	269	4.8	0	19.7	40.0	36.2	4.1	1.50	2.05
2	760	269	9.7	0	19.7	39.4	38.3	2.6	1.45	2.0
6	1110	269	6.8	0	27.8	40.4	29.7	2.0	2.15	1.45

<sup>a</sup> Overall conversion.

Table IV. Reactions of Isopentane over 10% Pt–Al<sub>2</sub>O<sub>3</sub> (Product Distributions)

Run	$P_{H_2}$	$T, ^\circ C$	$\alpha, \%$	5CH <sub>4</sub>	CH <sub>4</sub> + C <sub>4</sub> H <sub>10</sub>	C <sub>2</sub> H <sub>6</sub> + C <sub>3</sub> H <sub>8</sub>	<i>n</i> -C <sub>5</sub> H <sub>12</sub>	Neo-C <sub>5</sub> H <sub>12</sub>	$\rho_1$	$\rho_2$	$\rho_3$
11	760	262	8.3	0	46.1	14.6	33.3	6.0	1.80	0.3	1.2
12	760	276	7.5	0	35.9	15.2	42.9	5.9	1.05	0.4	1.15
13	760	276	4.2	0	34.4	13.4	46.2	6.0	0.90	0.4	1.1
14	760	286	4.9	0	26.0	14.3	53.9	5.7	0.70	0.55	1.15
15	760	292	8.3	0	26.0	16.3	52.1	5.6	0.75	0.65	1.3
16	295	276	8.6	1.4	14.4	15.3	63.7	5.2	0.45	1.05	1.05
17	293	276	7.5	2.2	14.9	15.7	61.8	5.4	0.45	1.05	1.00
12	760	276	7.5	0	35.9	15.2	42.9	5.9	1.05	0.4	1.15
18	1190	276	14.0	0	56.8	17.2	20.4	5.6	2.85	0.3	1.25

$$ba_{5b} + ca_{5c} + da_{5d} = a_5 \quad (9)$$

$$ba_{4b} + ca_{4c} + da_{4d} = a_4 \quad (10)$$

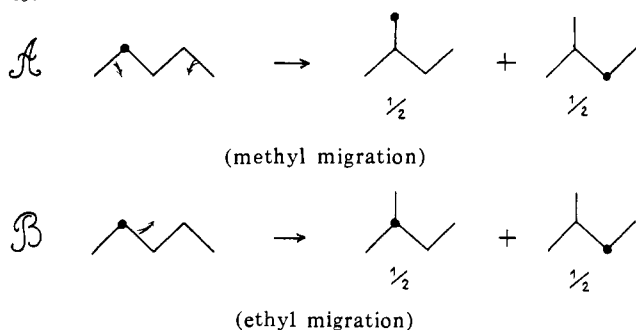
$$b + c + d = 1 \quad (11)$$

$$b = 2d \quad (12)$$

lated; the values found for  $|S - 1|$  reported in Table V are always less than  $0.1(b + d)$ , which is compatible with the experimental errors. It is therefore ascertained that isomerization via a cyclic mechanism is the major scrambling process. However, the accuracy of the measurements does not allow one to eliminate any other minor process, provided its contribution is less than 10%, or any isotopic effect.

From  $b$  and  $d$ , it is possible to deduce the conversion  $\alpha' = 2b + d$  for the scrambling reaction 8 and to compare with the conversion  $\alpha$  for the *n*-pentane  $\rightarrow$  isopentane isomerization 3. Both conversions  $\alpha$  and  $\alpha'$  are similar, but it is apparent from Table V that an increase in temperature or a decrease in hydrogen pressure favors the scrambling reaction vs. the chain shortening.

**Isopentanes.** The determination of the concentrations of the various isotopic varieties is much more accurate for the isopentanes ( $e, f, g$ , given in Table V) than for the *n*-pentanes, which allows one to calculate precisely, after having eliminated all the side-reaction products, the relative contributions of the two possible bond shift isomerizations  $\mathcal{A}$  and  $\mathcal{B}$ .



Scheme I shows the various consecutive and parallel reactions which lead to isopentane. Besides the molecules formed directly from *n*-pentane-2-<sup>13</sup>C ( $e_r, f_r, g_r$ ), isopentanes may appear as the result of consecutive reactions, either from the primary isopentanes by methyl shift 3, or by

chain shortening from the *n*-pentanes obtained from a cyclic mechanism 1 + 2'. In the latter case, the carbon-13 is distributed randomly among all the carbon atoms of the various *n*-pentane and isopentane molecules.

From the concentrations of the isomerized *n*-pentanes ( $x'$ ) and isopentanes ( $y + y'$ ), it is easy, assuming that each reaction 1, 2, and 2' is first order, to deduce the concentration  $y$  and the distribution  $e_0, f_0, g_0$  of the isotopic varieties for all the isopentanes, primary and secondary, obtained from *n*-pentane-2-<sup>13</sup>C by chain shortening.

In order to calculate the true initial distribution of isopentanes  $e_r, f_r, g_r$  from  $e_0, f_0, g_0$ , it is necessary to account for the isotopic effect  $1/\delta$  in the *n*-pentane  $\rightarrow$  isopentane isomerization and for the extent of the consecutive methyl shift.  $\delta$  is defined as the ratio between the rate of isomerization involving the break of a <sup>13</sup>C-<sup>12</sup>C and that of a <sup>12</sup>C-<sup>12</sup>C bond. It may be obtained from the experimental ratios  $R_{5i}$  and  $R_{5p}$  (<sup>13</sup>C<sup>12</sup>C<sub>4</sub>H<sub>12</sub><sup>+</sup>/<sup>12</sup>C<sub>5</sub>H<sub>12</sub><sup>+</sup> between the heavy and light parent ions in isopentane and *n*-pentane, respectively).

$$R_{5i} = R_{5p}[(1 + \delta)/2]$$

The mean value of  $1/\delta$  is  $1.10 \pm 0.02$  for seven experiments (Table VI). From  $1/\delta$  and ( $e_0, f_0, g_0$ ) one may calculate the true initial distribution by solving the system of four equations.

$$\begin{aligned} (1) \quad e_0 &= e_r(1 - \beta/2) \\ (2) \quad f_0 &= \beta g_r + (1 - \beta)f_r \\ (3) \quad g_0 &= (1 - \beta)g_r + \beta f_r + (\beta/2)e_r \\ (4) \quad (A + B) &= f_r(1 + \delta) + e_r(1 + 1/\delta) = 1 \end{aligned} \quad (II)$$

Equations II-1 to II-3 are immediately obtained from Scheme I. The normalizing eq II-4 may be deduced from eq III which expresses the true initial distribution  $e_r, f_r, g_r$  as a function of  $\delta$  and the isomerization rates  $r_A, r_B$  of a light molecule according to the bond shift mechanisms  $\mathcal{A}$  and  $\mathcal{B}$ . Except for one experiment at low temperature,  $\beta$  is quite large (around 20%), which suggests that methyl shift is a very fast reaction, when compared with both the cyclic *n*-pentane  $\rightarrow$  *n*-pentane isomerization, and the *n*-pentane  $\rightarrow$  isopentane isomerization.

Table V. Isomerization of Pentane-2-<sup>13</sup>C (Distribution of the Various Isotopic Varieties)

Run	Catalyst sample	T, °C	P <sub>H<sub>2</sub></sub>	α, %	α', %	n-Pentanes			Isopentanes				
						b	c	d	(S-1)	e	f	g	g
21	a	281	760	4.9	8.5	0.034	0.951	0.017	0.002	0.126	0.401	0.473	0.478
22	b	296	760	4.3	5.0	0.020	0.970	0.010	0.000	0.123	0.399	0.478	0.478
23	b	281	760	3.7	2.65	0.010	0.983	0.005	-0.002	0.121	0.397	0.482	0.482
24	b	269	760	3.7	2.15	0.008	0.987	0.004	-0.001	0.117	0.397	0.485	0.485
25	c	281	272	4.6	14.1	0.056	0.912	0.028	-0.004	0.153	0.378	0.469	0.469
26	c	281	760	3.7	2.15	0.008	0.987	0.004	-0.001	0.115	0.406	0.479	0.479
27	c	281	1070	3.1	1.0	0.004	0.995	0.002	0.001	0.123	0.397	0.480	0.480

Table VI. Isomerization of n-Pentane to Isopentane (Relative Contributions of Bond Shift Mechanisms and Isotopic Effect)

	Run						
	21	22	23	24	25	26	27
β, %	27.4	18.1	12.8	0	27.2	18.3	22.9
A, %	27.1	26.45	26.8	24.1	32.2	26.0	26.45
1/δ	1.10	1.11	1.08	1.08	1.09	1.08	1.12

$$e_r = \frac{r_A \delta}{(r_A + r_B)(1 + \delta)}$$

$$f_r = \frac{r_B}{(r_A + r_B)(1 + \delta)}$$

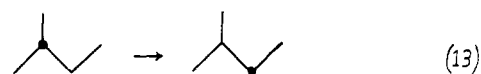
$$g_r = \frac{r_A + r_B \delta}{(r_A + r_B)(1 + \delta)} \quad (\text{III})$$

$$A = \frac{r_A}{r_A + r_B} = e_r(1 + 1/\delta)$$

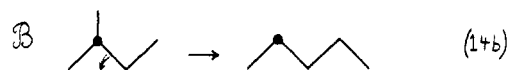
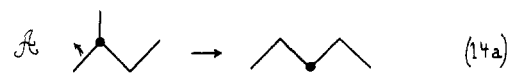
$$B = \frac{r_B}{r_A + r_B} = f_r(1 + \delta)$$

With the exception of the experiment carried out at a very low hydrogen pressure, *A* remains fairly constant (26 ± 2%). The experimental conditions, temperature and hydrogen pressure, do not seem to greatly affect the relative importance of the two bond shift mechanisms  $\mathcal{A}$  and  $\mathcal{B}$ .

(III) Isomerization of 2-Methylbutane-2-<sup>13</sup>C. In order to investigate the methyl shift and to compare with the isopentane → *n*-pentane isomerization, the contact reactions of 2-methylbutane-2-<sup>13</sup>C (2MB-2-<sup>13</sup>C) on 10% Pt-Al<sub>2</sub>O<sub>3</sub> have been studied under various experimental conditions. The labeling of the molecule allows one to distinguish between three elementary reactions: methyl shift



Chain lengthening according to bond shifts

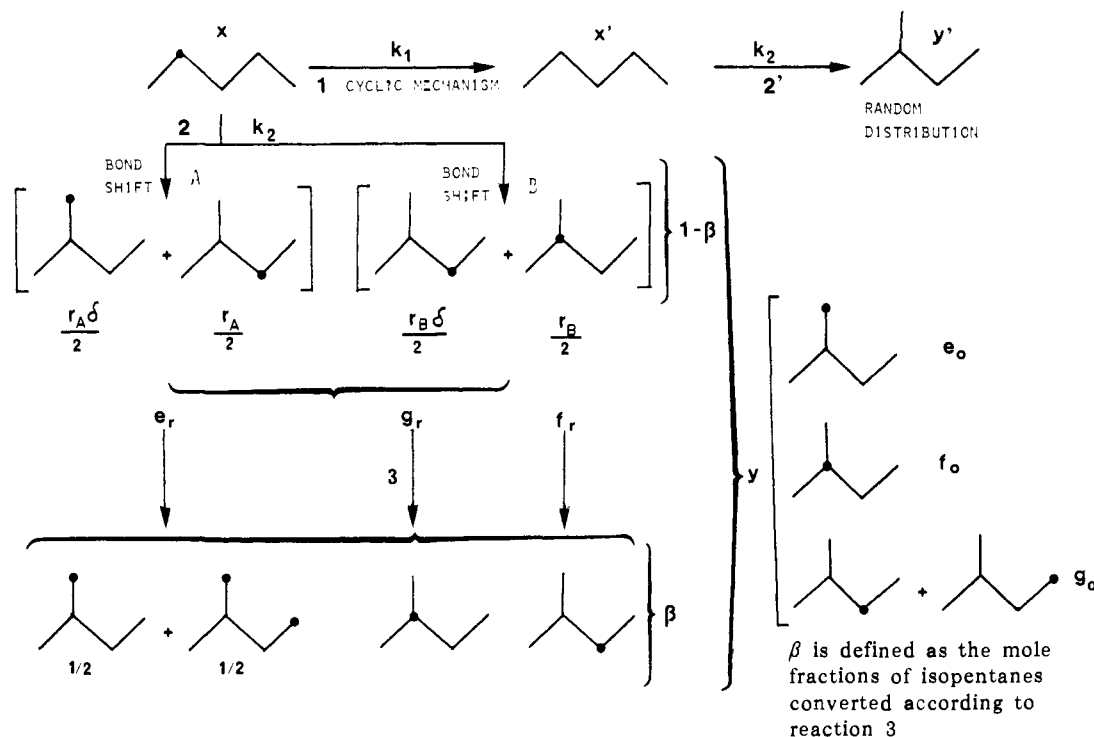


The product distributions for isopentanes and pentanes are given in Table VII. The conversion  $\alpha'$  for reaction 13, measured by the amount of 2-MB-3-<sup>13</sup>C, is always larger, by a factor of 3 to 6, than the conversion  $\alpha$  for the isopentane → pentane isomerization. The ratio  $\alpha'/\alpha$  depends on temperature and hydrogen pressure, but not on hydrocarbon pressure. Also in Table VII the ratio  $R_{Si}/R_{Sp}$  is given, which measures the isotope effect for the isopentane → *n*-pentane isomerization. A mean value of 1.07 was found, slightly lower than that obtained for the reverse reaction.

Since methyl shift is fast when compared with isomerization to *n*-pentane, an accurate estimate of mechanisms  $\mathcal{A}$  and  $\mathcal{B}$  requires corrections taking account of this speedy reaction. Similarly the consecutive isomerization via a cyclic intermediate, proven by the presence of small but definite amounts of *n*-pentane-1-<sup>13</sup>C in the reaction products, should also be considered. The various consecutive and parallel reactions are summarized in Scheme II.

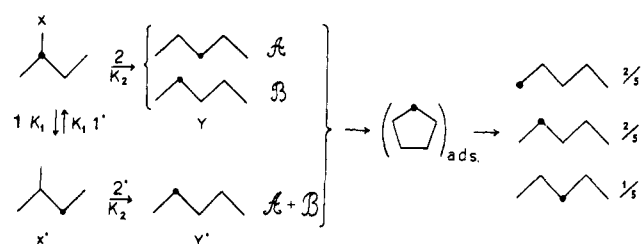
All reactions are assumed to be first order vs. hydrocarbon and the *n*-pentane → isopentane isomerization is neglected. It will be assumed also that the isotope effects are the same for steps 1 and 1' and 2 and 2'. With these as-

Scheme I

Table VII. Isomerization of Methyl-2-butane-2-<sup>13</sup>C (Distribution of the Isotopic Varieties)

Run	Cat. sample	$P_{H_2}$ , Torr	$P_{HC}$ , Torr	$T$ , °C	$\alpha$ , %	$\alpha'$ , %	$1/\delta$	<i>n</i> -Pentanes			Isopentanes			$A_r$ , %
								b	c	d	e	f	g	
31	e	5	760	289	4.5	24.4	1.07	0.000	0.785	0.215	0	0.244	0.756	24.9
32	g	6	760	289	5.4	24.3	1.13	0.047	0.737	0.216	0	0.243	0.757	27.0
33	e	40	760	289	5.5	27.4	1.05	0.002	0.787	0.211	0	0.274	0.726	25.2
34	g	6	760	275	5.6	27.6	1.04	0.000	0.770	0.230	0	0.276	0.724	25.3
35	g	6	760	307	7.0	19.2	1.06	0.054	0.710	0.236	0	0.192	0.808	27.0
36	g	6	295	289	8.3	21.2	1.05	0.097	0.669	0.234	0	0.212	0.788	27.8
37	g	6	1164	289	6.2	27.6	1.07	0.000	0.780	0.220	0	0.276	0.724	26.0

Scheme II



sumptions, the *initial* distribution of the isotopic varieties of pentanes (*c*, *d*, *r*) are calculated from the observed ones (*b*, *c*, *d*) first by taking into account the scrambling process and then by eliminating the *n*-pentanes formed by the successive reactions 2'.

The contributions  $A = d_r$  and  $B = c_r$  of both bond shift mechanisms are reported in the last columns of Table VII. The values found  $A$  ( $26 \pm 2$ ) approximate closely to the value of  $A$  found for the reverse reaction (*n*-pentane  $\rightarrow$  isopentane isomerization).

(IV) **Isomerization and Hydrocracking. Kinetic Data.** When *n*-pentane or isopentane is put in contact with a Pt- $Al_2O_3$  catalyst, a number of reactions take place: chain lengthening or shortening, methyl shift, demethylation, internal fission, *n*-pentane  $\rightarrow$  *n*-pentane isomerization. Some

of these reactions can only be recognized by using labeled hydrocarbons. In order to determine the "parent" reactions, i.e., the ones involving a common intermediate, the knowledge of kinetic data such as apparent activation energies and orders vs. hydrogen or hydrocarbon is required.

**Activation Energies.** The apparent activation energies  $E_a$  have been determined for the various contact reactions of pentane-2-<sup>13</sup>C and 2-methylbutane-2-<sup>13</sup>C; they are reported in Table VIII, together with the corresponding frequency factors  $A$ . While the determination of  $E_a$  is very accurate for isomerization, as shown in Figure 3, it is not so good for the hydrogenolysis reactions.

According to Table VIII, the activation energies allow the classification of the different reactions into four groups: (a) the *n*-pentane  $\rightarrow$  *n*-pentane isomerization according to a cyclic mechanism (ca. 70 kcal/mol); (b) the isomerization of *n*-pentane to isopentane and the reverse reaction (ca. 55 kcal/mol); (c) a group of reactions including methyl shift, isomerization of isopentane to neopentane, and hydrocracking of an internal C-C bond (ca. 45 kcal/mol); (d) demethylation (ca. 35 kcal/mol).

**Hydrogen Pressure Dependency.** From the plots  $\log r = f(\log P_{H_2})$  (Figure 4), the orders vs. hydrogen,  $-b$ , could be determined with good accuracy for the following reactions: *n*-pentane  $\rightarrow$  *n*-pentane isomerization, demethylation of isopentane, and isomerization of isopentane to *n*-pentane

Table VIII. Isomerization and Hydrogenolysis (Kinetic Data)

Reactions	$E_a$ , kcal/mol	$\log A^a$	$b$
	$71.4 \pm 1.5$	$21 \pm 0.5$	$-3.4 \pm 0.1$
	$55.3 \pm 1.5$	$14.7 \pm 0.5$	$-1.8 \pm 0.1$
	$44.5 \pm 3$	$10.5 \pm 1$	$-1.3 \pm 0.2$
	$38.5 \pm 3$	$7.5 \pm 1$	$-0.6 \pm 0.2$
	$54.3 \pm 1.5$	$14.4 \pm 0.5$	$-2.3 \pm 0.15$
	$45.3 \pm 1.5$	$9.9 \pm 0.5$	$-1.9 \pm 0.2$
	$45 \pm 3$	$10.4 \pm 1$	$-1.65 \pm 0.15$
	$45 \pm 3$	$10.8 \pm 1$	$-1.65 \pm 0.2$
	$35 \pm 3$	$2.5 \pm 1$	$-0.7 \pm 0.1$

<sup>a</sup> $A$  is expressed in mol/sec  $\times$  g of catalyst.

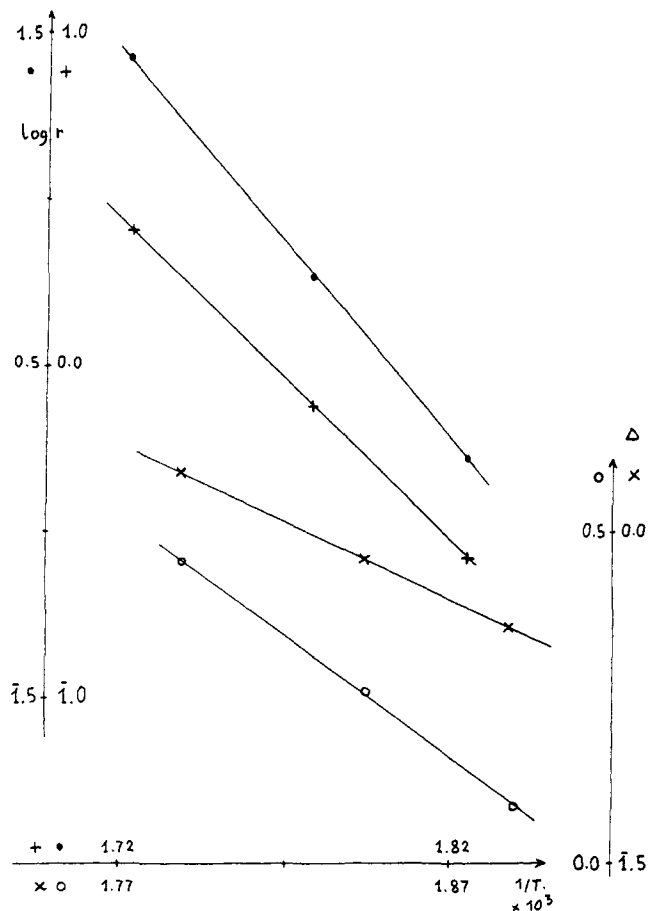


Figure 3. Apparent activation energies of isomerization and hydrogenolysis reactions.  $\log r = f(1/T)$  plots for the isomerization of: 2-methylbutane-2-<sup>13</sup>C to *n*-pentane (•) and 2-methylbutane-2-<sup>13</sup>C to 2-methylbutane-3-<sup>13</sup>C (+).  $\Delta$ :  $\log r_2/r_1 = f(1/T)$  plots:  $r_2$  = isomerization rate of isopentane to *n*-pentane,  $r_1$  = rate of internal fission (X) and demethylation (O) of 2-methylbutane.

and the reverse reaction. The determinations of the order vs. hydrogen were not so good for the isomerization of isopentane to neopentane and for the hydrogenolysis of the internal C-C bond of isopentane.

The orders vs. hydrogen, always negative, are given in the last column of Table VIII; they allow one to classify the isomerization reactions roughly in two groups: the *n*-pentane  $\rightarrow$  *n*-pentane isomerization (with a highly negative order of  $-3.4$ ) and the other reactions, with an order close to  $-2$ . This classification corresponds to that which could have been made according to the two proposed mechanisms, cyclic or bond shift. However, the difference between the

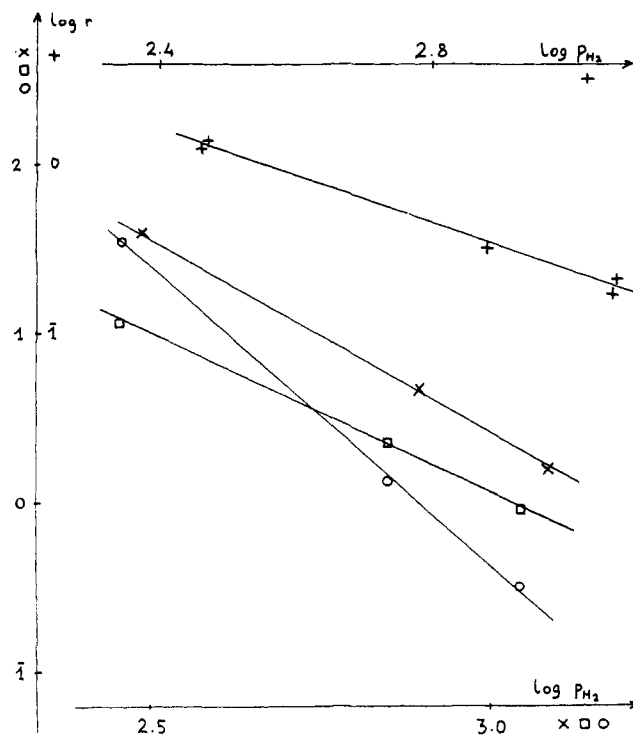


Figure 4. Hydrogen pressure dependency.  $\log r = f(\log P_{H_2})$  plots: demethylation of 2-methylbutane (+); isomerization of *n*-pentane to 2-methylpentane ( $\square$ ); isomerization of *n*-pentane to *n*-pentane (O); isomerization of 2-methylbutane to *n*-pentane (X).

orders of, say, the isopentane  $\rightarrow$  *n*-pentane isomerization ( $-2.3$ ) and the reverse reaction ( $-1.8$ ) is far beyond the experimental errors.

Among the hydrogenolysis reactions, the demethylations of isopentane and *n*-pentane are associated with a high order vs. hydrogen ( $-0.6$ ). On the contrary the orders for the internal fission are much more negative; they are only one-half unit higher than the ones found for the isomerization of the corresponding hydrocarbons isopentane  $\rightarrow$  *n*-pentane and *n*-pentane  $\rightarrow$  isopentane.

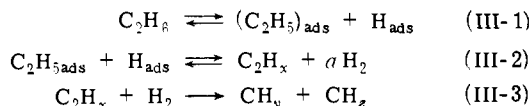
An interesting feature which appears from Table VIII is the correlation which exists between the apparent activation energies and the orders vs. hydrogen for all the contact reactions of *n*-pentane and isopentane. The more negative the order, the higher is the activation energy.

#### Discussion

One of the most striking results of this study is the very high negative orders vs. hydrogen found for all the hydrogenolysis and isomerization reactions. Negative orders were

found previously for the hydrogenolysis of hydrocarbons on metals and especially of ethane.<sup>22-29</sup> The kinetics data have been most generally interpreted by using a treatment first proposed by Cimino, Boudart, and Taylor.<sup>24</sup> This treatment, summarized by Scheme III, implies a progressive de-

Scheme III



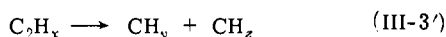
hydrogenation of the adsorbed molecule, forming a series of species in equilibrium, one of which is involved in the rupture of the carbon-carbon bond (III-3). Provided this rupture is the rate-determining step and equilibrium is completed for reactions III-1 and III-2, the rate may be expressed as

$$r = k \frac{(KP_{\text{C}_2\text{H}_6}/P_{\text{H}_2})^a P_{\text{H}_2}}{1 + KP_{\text{C}_2\text{H}_6}/P_{\text{H}_2}^a}$$

where  $a = (6 - x)/2$ , which approximates to

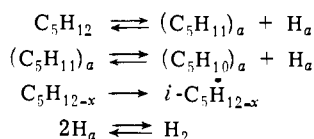
$$r \approx k' P_{\text{C}_2\text{H}_6}^n P_{\text{H}_2}^{1-na} \quad (15)$$

According to (15) a negative order vs. hydrogen of  $-b$  would then correspond to the removal of a minimum of  $2a = 2 + 2b$  hydrogen atoms ( $2 + 2b$ )/ $n$  in fact) from the molecule before the hydrogenolysis takes place. A modification of this treatment has been proposed by Sinfelt and associates,<sup>30</sup> who assumed that on some metals such as cobalt and rhenium, where C-H and C-C bond ruptures (or formations) are of comparable rates, equilibrium III-1 was no longer attained. Provided a stationary state is reached for ethyl radicals, the order vs. hydrogen should vary in this case between 0 and  $1 - a$ , according to temperature and hydrogen pressure. Here again  $2 + 2b$  represents the minimum number of hydrogens removed from the molecule to form the reactive species. This figure is lowered to  $2b$  if the bimolecular cracking reaction III-3 is replaced by an unimolecular decomposition III-3'.<sup>31,23</sup>



The isomerization of pentanes could be interpreted in a similar way. In Scheme III' it is assumed that each hydrogena-

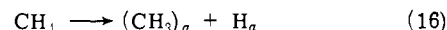
Scheme III'



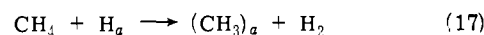
tion step is unimolecular, in equilibrium, and that the rate-determining step is the isomerization reaction. Accordingly a negative order of  $-b$  means that  $2b$  hydrogen atoms at least have been removed from the molecule before the skeletal rearrangement takes place. The high negative orders found for the various reactions would imply then that *four* to *seven* hydrogen atoms have been taken away when forming the precursor for bond shift or cyclic type isomerization. This seems really unlikely. In the case of ethane hydrogenolysis, the values found for  $-b$  led to the conclusion that the species  $\text{C}_2\text{H}_x$  were extremely poor in hydrogen (mainly dicarbon species  $\text{C}_2$ ), but this hydrogen deficiency could in some way be considered as the driving force for the rupture of the carbon-carbon bond. Such a consideration does not hold in the case of skeletal rearrangement, where the product is desorbed as a complete molecule and not as small  $\text{C}_1$  fragments. The classical mechanism represented in Scheme

III' does not therefore seem adequate to explain the isomerization reactions.

Some years ago, a very interesting proposal was made by Frennet and associates<sup>32</sup> that the adsorption of methane at high temperature did not proceed by the formation of methyl adsorbed radicals according to a simple unimolecular reaction



but according to a bimolecular reaction between gaseous methane and adsorbed hydrogen



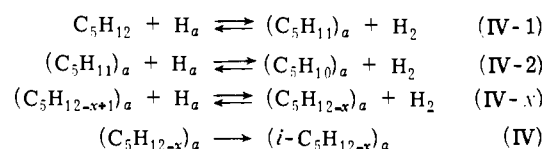
By using the very same eq 17 and by assuming moreover that the surface coverage in hydrogen  $\theta_{\text{H}}$  depended mainly upon the surface coverage in hydrocarbon  $\theta_{\text{C}}$  and remained therefore practically constant

$$\theta_{\text{H}} = \theta_{\text{H}_0}(1 - \theta_{\text{C}})$$

Frennet and Lienard<sup>33</sup> were able to interpret the variations of the surface composition in carbon and hydrogen atoms during the coadsorption of hydrogen and methane on rhodium films in a very broad pressure range.

The same concept as the one used for the methane-hydrogen system may be used for skeletal rearrangement. Let us assume that the rate-determining step in isomerization involves a species  $\text{C}_5\text{H}_{12-x}$  whose formation requires a series of bimolecular reactions such as 17 in equilibrium. According to Scheme IV, the rate of isomerization may be ex-

Scheme IV



pressed as follows

$$v = k\theta_{\text{C}_5\text{H}_{12-x}} = k \prod_i K_i \frac{P_{\text{C}_5\text{H}_{12}} \theta_{\text{H}}^x}{P_{\text{H}_2}^x} \approx \frac{k \prod_i K_i P_{\text{C}_5\text{H}_{12}} \theta_{\text{H}_0}^x}{P_{\text{H}_2}^x} \quad (18)$$

since  $\theta_{\text{H}} = \theta_{\text{H}_0}(1 - \theta_{\text{C}}) \approx \theta_{\text{H}_0}$ , where  $k$  represents the rate constant and  $K_i$  the equilibrium constant for the  $i$ th chemical equation IV- $i$ . According to (18), a negative order of  $-b$  would mean that  $b$  hydrogen atoms (and not  $2b$ ) have been removed from the molecule to form the species precursor of the isomerization process. The orders vs. hydrogen for the cyclic type isomerization and for bond shift being close to  $-4$  and  $-2$ , respectively, Scheme IV, would mean then that *four* and *two* hydrogen atoms (and not eight and four) are taken away from the pentane molecule when forming the precursor species.

It is interesting to emphasize that the sequence of reactions IV explains not *only* the very high negative orders vs. hydrogen, *but also* the large apparent activation energies found for isomerization and the correlation which has been observed between the orders and the apparent activation energies and entropies,  $E_a$  and  $\Delta S_a$ .

From eq 18 the following may easily be derived

$$\begin{aligned} E_a &= E + \sum \Delta H_i \\ \Delta S_a &= \Delta S^\ddagger + \sum \Delta S_i \end{aligned}$$

where  $E$  and  $\Delta S^\ddagger$  represent the true activation energy and entropy for the surface reaction.  $\Delta H_i$  and  $\Delta S_i$  are the enthalpy and entropy change for the chemical equation IV- $i$ .

The enthalpy change in IV- $i$ , from left to right, is roughly equal to the difference between the bond energies of a



metal-hydrogen bond  $D_{Me-H}$  and a metal-carbon bond  $D_{Me-C}$ . Indeed:

$$\Delta H \approx -D_{H-H} + D_{C-H} + D_{Me-H} - D_{Me-C} \approx D_{Me-H} - D_{Me-C} - 4 \text{ kcal/mol}$$

With a heat of hydrogen adsorption of ca. 30 kcal/mol, the metal-hydrogen bond energy may be estimated around 60–70 kcal/mol, which is much higher than the bond energy of any metal-carbon bond.<sup>34</sup> The enthalpy change  $\Delta H_i$  for each reaction IV-*i* is therefore substantially positive. (The only comparison between metal-hydrogen and metal-carbon bond energies available for the same metal concerns beryllium. Values of 79 and 45 kcal/mol have been found for  $D_{Be-H}$  and  $D_{Be-C}$ , respectively.<sup>35</sup>) Since these enthalpy changes are added to the true activation energy, one expects very high apparent activation energies for the isomerization reactions. Moreover, the more numerous the equilibrium reactions in Scheme IV, and consequently the more negative the orders vs. hydrogen, the higher is the apparent activation energy, as in fact was observed. (A similar correlation between apparent activation energy and order vs. hydrogen has already been observed by Sinfelt and associates for the hydrogenolysis of ethane on various metals.<sup>28</sup> This result was interpreted by assuming that the overall equilibrium reaction  $C_2H_6 \rightleftharpoons C_2H_x + aH_2$  (III-1 and III-2) was endothermic from left to right.)

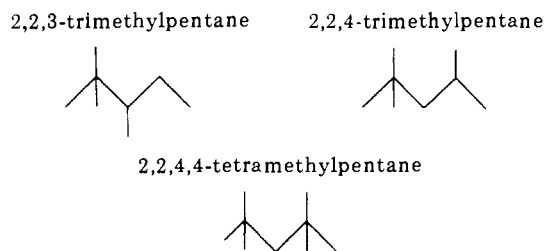
Similar considerations also explain the paradoxical result that the apparent activation entropy is larger for the cyclic type isomerization than for bond shift. All the eq IV-*i*, except the first one, are associated with an increase of the translational degrees of freedom, and therefore with a positive change of entropy  $\Delta S_i$ . Hence, although the true activation entropy is probably smaller for cyclic rearrangement than for bond shift, on account of geometrical requirements, the number of the steps in equilibrium, and consequently  $\Sigma \Delta S_i$  and the apparent activation entropy, would be expected to be larger for the former than for the latter reaction.

Although the systematic use of bimolecular surface reactions in Scheme IV explains most of the results presented here, i.e., high negative orders vs. hydrogen, abnormally large apparent activation energies, and interrelationship between both sets of kinetic data, several restrictions should be put forward. First the orders  $-b$  vs. hydrogen are never exact integers, which would mean, according to eq 2, that  $\theta_H$  might be somewhat pressure dependent. The number of hydrogen atoms removed from the molecule to form the precursor should be taken then as equal to the first integer number larger than  $b$ .

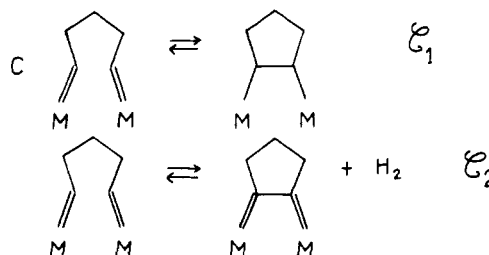
A more severe limitation lies in the systematization of the simpler Frennet mechanism. First it is quite possible that these reactions which have their counterpart in homogeneous catalysis, such as interconversions in  $\sigma$ -alkyl,  $\pi$ -olefinic, and  $\pi$ -allylic species, are unimolecular as described in Scheme III'. Secondly a more satisfactory way to represent the multiple adsorption and to interpret the results would be to imagine the hydrocarbon, and the hydrogen on the surface below it, as a van der Waals complex, with successive C-M chemical bonds formed by the loss of molecular hydrogen. In the kinetic treatment, the whole assembly could be viewed as one molecule and a rate expression similar to eq 18, with the  $\theta_H$  values removed, would be obtained. (We thank one of the referees for having suggested this mechanism.)

(V) **Reaction Mechanisms.** If one assumes that the precursor species leading to the cyclic intermediate are formed only by bimolecular reactions, according to Scheme IV, the observed order vs. hydrogen,  $-3.6$ , would correspond to the

removal of four hydrogen atoms. Moreover, it was shown previously<sup>36</sup> that the dehydrocyclization rates of several substituted pentanes, i.e.,



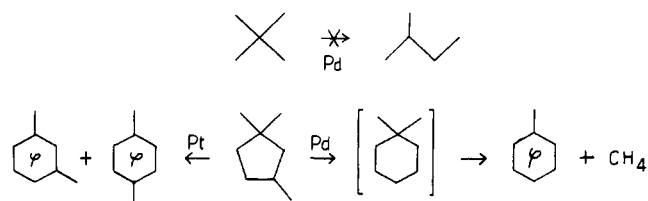
are equal, which demonstrates that only the *terminal* carbon atoms 1 and 5 are adsorbed in the precursor species C. From these results, it follows that C is an 1,1,5,5-tetraadsorbed species and, according to whether hydrogen is involved or not in the reverse reaction, i.e., hydrogenolysis of cyclopentane, two mechanisms  $\mathcal{C}_1$  and  $\mathcal{C}_2$  may be proposed



for the dehydrocyclization. From these two mechanisms, the first one seems a priori much more simple. However, the second one accounts for the sharp selectivity observed in the hydrogenolysis of the various C-C bonds of methylcyclopentane on 10% Pt-Al<sub>2</sub>O<sub>3</sub> and platinum films; on these catalysts *n*-hexane is formed in very small amounts.<sup>37</sup>

**Bond Shift and Hydrogenolysis.** According to their apparent activation energies, the bond shift isomerizations may be classified into two groups. The first group (I) is made up of isomerization of isopentane to *n*-pentane and the reverse reaction ( $E_a = 55$  kcal/mol). The second group (II) is methyl shift and formation of neopentane ( $E_a = 45$  kcal/mol). The same apparent activation energy and order vs. hydrogen are also found for the internal fission of *n*-pentane and isopentane. It will therefore be assumed that the same reaction mechanism is involved for these two hydrogenolysis reactions and the two isomerization reactions of the second group. On the contrary, a different mechanism will be envisaged for the *n*-pentane  $\rightarrow$  isopentane isomerizations.

It is interesting at this stage to underline the specificity of platinum in the four reactions of group II. On palladium, which is the second best metal catalyst for isomerization, skeletal rearrangement does not occur within a quaternary carbon atom; neopentane is not isomerized on palladium<sup>7</sup> and the aromatization of 1,1,3-trimethylcyclopentane involves a ring enlargement at the tertiary carbon atom, and



not at the quaternary one as on platinum.<sup>16</sup> Similarly, on palladium, methyl shift is a minor reaction and the internal fission is negligible.<sup>20</sup>

The common precursor for the four reactions of group II should therefore be highly specific of platinum. We suggest

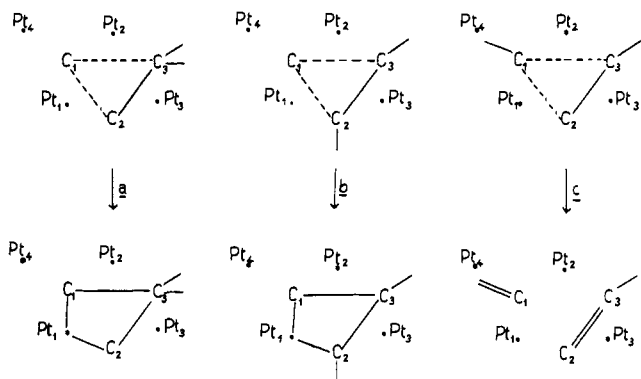
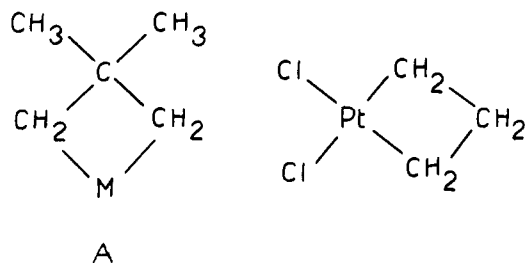
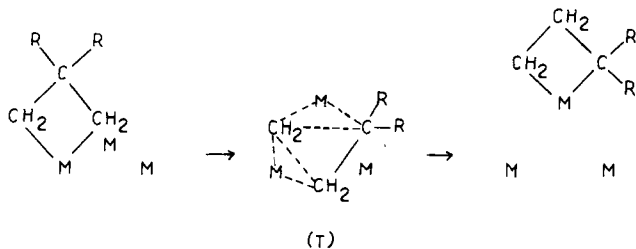


Figure 5.

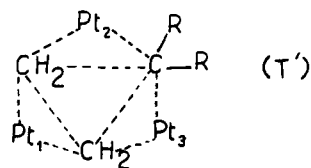
that this precursor is an  $\alpha\gamma$  diadsorbed species A similar to the trimethylene di- $\sigma$ -complex of platinum. Such a complex is formed reversibly by reacting cyclopropane and chloroplatinic acid<sup>38</sup> and has no analog with any other metal. The



transfer of the organic moiety to a second superficial platinum atom via a transient species T, where a quasi-cyclopropane intermediate lying almost flat on the surface is loosely bonded to two metal atoms, could explain the isomerization



This mechanism, with respect to the previous ones, presents many advantages. (1) The removal of two hydrogen atoms to form the precursor is in good agreement with the observed order (-1.7) according to Scheme IV. (2) The (111) face of platinum is known to favor isomerization.<sup>9</sup> As shown in Figure 5, the cyclopropane structure of the transient species T fits nicely with the geometry of this face. It is even possible that three and not two metal atoms interact with the organic variety (T'). (3) The geometry of the transient



species explains also why methyl shift, formation of neopentane, and *not* isopentane  $\rightarrow$  *n*-pentane isomerization are possible by this mechanism. Figure 5 shows the transient species for the three reactions (a, b, c). In each case the C<sub>1</sub>-C<sub>2</sub> bond is weakened and the C<sub>1</sub>-C<sub>3</sub> bond not yet completely formed. A part of the transient species, CH<sub>2</sub> in the first two reactions and CH<sub>3</sub>-CH in the third, is therefore temporarily removed from the remainder of the molecule and may interact with a fourth platinum atom Pt<sub>4</sub> in the vi-

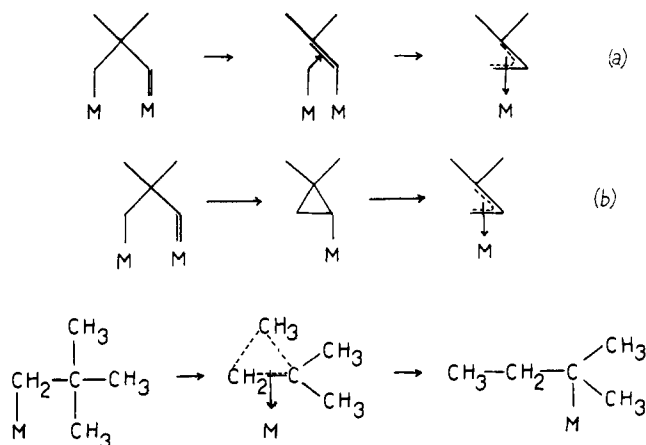


Figure 6.

city. The difference between the two situations (3a) or (3b) and (3c) is that the bonding of CH<sub>2</sub> with Pt<sub>4</sub> is loose enough, while a simple hydrogen shift transforms CH<sub>3</sub>-CH into an adsorbed ethylene molecule. In Figure 5c, the bond shift is therefore replaced by a rupture of the molecule yielding ethane and propane. Thus it is shown simultaneously that the same mechanism explains internal fission and methyl shift but cannot account for the isopentane  $\rightarrow$  *n*-pentane isomerization.

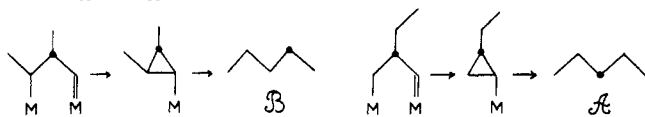
It is worthwhile to note that internal fission requires a greater number of metal atoms than bond shifts. It is therefore not surprising that on a dispersed catalyst such as the 0.2% Pt-Al<sub>2</sub>O<sub>3</sub> internal fission has no longer the same apparent activation energy and order vs. hydrogen as the bond shift reactions, but instead the same as demethylation.<sup>39</sup> It occurs by an entirely different mechanism.

In order to interpret the isopentane  $\rightarrow$  *n*-pentane isomerization, one could suggest one of the three major mechanisms which have been proposed previously for the bond shift reactions, as little founded on fact as they might be. Two of them involve  $\alpha\gamma$  triadsorbed species as precursors. While Anderson and Avery suggest a  $\pi$ -complex intermediate (Figure 6a),<sup>15</sup> an adsorbed cyclopropane intermediate is proposed by Gault et al.<sup>16</sup> The third mechanism, proposed recently by Rooney et al.,<sup>17</sup> assumes a 1-2 alkyl shift in an adsorbed alkyl radical, via a transient species involving three center orbitals as in the nonclassical carbonium ions (Figure 6c). Rooney's mechanism explains nicely the rearrangements occurring on platinum and palladium in the cage molecules (substituted adamantane and so on) but cannot be applied to the pentane system; indeed it would imply a minimum order vs. hydrogen of -1, while values between -1.8 and -2.3 are obtained.

The cyclopropane and the  $\pi$ -complex mechanisms seem more suitable for the *n*-pentane  $\rightarrow$  isopentane isomerizations; they are consistent with the observed orders vs. hydrogen and are both dissymmetrical, which could account for the slight but definite differences between the orders for the direct and the reverse reaction.

It is difficult to choose between the two above mechanisms; according to the cyclopropane mechanism, no hydrogenolysis reaction should be associated with the bond shift reaction, as in fact is observed, while the reverse is true of the  $\pi$ -complex mechanism, as pointed out by Anderson himself.<sup>9</sup> A second reason to prefer the cyclopropane mechanism is that it explains easily, by the relative stability of the cyclic intermediate, the predominance of bond shift  $\beta$  over bond shift  $\alpha$ . Ab initio calculations have shown that there is a difference of 10 kcal/mol between the energy levels of cyclopropane and dimethylcyclopropane,<sup>40</sup> which

could explain the relative ease of the two skeletal rearrangements  $\alpha$  and  $\beta$ .



### Conclusion

The combination of kinetic and tracer studies gives some ideas on the various reactions occurring on a platinum surface. *The first conclusion* concerns the number of parallel reactions involved simultaneously. Previous work<sup>37</sup> had shown the existence of two cyclic mechanisms for the isomerization of alkanes: the nonselective and the selective cyclic mechanism, which involves or not the formation and rupture of a tertiary-secondary CH<sub>2</sub>CH bond. From the present work, it appears that also two types of bond shift mechanisms exist. Similarly, hydrogenolysis occurs by at least two mechanisms. *The second main conclusion* is that, in the temperature range where skeletal rearrangement takes place, the classical unimolecular model of adsorption does not seem to be valid any more, and instead it is bimolecular elementary reactions that take place. The existence of such reactions which have no counterpart in homogeneous catalysis could very well explain the difference between metal surfaces and organometallic complexes in their ability to activate the carbon-hydrogen bond of saturated hydrocarbons.

**Acknowledgments.** We wish to thank Mrs. S. Corolleur for her help in the syntheses of the labeled hydrocarbons.

### References and Notes

- (1) B. A. Kazanskii, *Ouspikhi Khimii*, **17**, 655 (1948).
- (2) B. A. Kazanskii, A. L. Liberman, J. F. Bulanova, V. T. Aleksanlan, and Kh. E. Sterin, *Dokl. Akad. Nauk SSSR*, **95**, 77 (1954); **95**, 281 (1954).
- (3) A. L. Liberman, T. V. Lapshina, and B. A. Kazanskii, *Dokl. Akad. Nauk SSSR*, **105**, 727 (1955).
- (4) A. L. Liberman, O. V. Brazin, and B. A. Kazanski, *Dokl. Akad. Nauk SSSR*, **111** 1039 (1956); **129**, 578 (1959); **148**, 338(1963); *Izv. Akad. Nauk SSSR*, 879 (1959).
- (5) A. L. Liberman, K. K. Schnabel, T. V. Vasina, and B. A. Kazanskii, *Kinet Katal.*, **2**, 446 (1961); *Dokl. Akad. Nauk SSSR*, **117**, 430 (1957).
- (6) G. A. Mills, H. Heinemann, T. M. Milliken, and A. G. Oblad, *Ind. Eng. Chem.*, **45**, 134 (1953).
- (7) J. R. Anderson and B. G. Baker; (a) *Nature (London)*, **187**, 937 (1960); (b) *Proc. R. Soc. London, Ser. A*, **271**, 402 (1963).
- (8) Y. Barron, G. Maire, D. Cornet, J. M. Muller, and F. G. Gault: (a) *J. Catal.*, **2**, 152 (1963); (b) *ibid.*, **5**, 428 (1966).
- (9) J. R. Anderson and N. R. Avery, *J. Catal.*, **5**, 446 (1966).
- (10) (a) J. R. Anderson, R. J. McDonald, and Y. Shimoyama, *J. Catal.*, **20**, 147 (1971); (b) J. R. Anderson and Y. Shimoyama, *Catal., Proc. Int. Congr., 5th*, 695 (1973).
- (11) V. Ponc and W. M. H. Sachtler, *Catal., Proc. Int. Congr.*, 645 (1973).
- (12) C. Corolleur, S. Corolleur, and F. G. Gault, *J. Catal.*, **24**, 385 (1972).
- (13) C. Corolleur, D. Tomanova, and F. G. Gault, *J. Catal.*, **24**, 406 (1972).
- (14) C. Corolleur, F. G. Gault, D. Juttard, G. Maire, and J. M. Muller, *J. Catal.*, **24**, 406 (1972).
- (15) J. R. Anderson and N. R. Avery, *J. Catal.*, **7**, 315 (1967).
- (16) J. M. Muller and F. G. Gault, Symposium on Mechanisms and Kinetics of Complex Catalytic Reactions, Paper No. 15, Moscow, 1968.
- (17) M. A. McKervey, J. J. Rooney, and N. G. Samman, *J. Catal.*, **30**, 330 (1973).
- (18) C. Corolleur, S. Corolleur, and F. G. Gault, *Bull. Soc. Chim. Fr.*, 842 (1969).
- (19) J. E. Benson and M. Boudart, *J. Catal.*, **4**, 704 (1965).
- (20) M. Hajek, S. Corolleur, C. Corolleur, G. Maire, A. O'Connide, and F. G. Gault, *J. Chim. Phys. Phys.-Chim. Biol.*, **71**, 1329 (1974).
- (21) W. A. Dietz, *J. Gas Chromatogr.*, **68** (1967).
- (22) (a) K. Morikawa, W. S. Benedict, and H. S. Taylor, *J. Am. Chem. Soc.*, **58**, 1795 (1936); (b) K. Morikawa, N. R. Trenner, and H. S. Taylor, *ibid.*, **59**, 1103 (1937).
- (23) C. Kemball and H. S. Taylor, *J. Am. Chem. Soc.*, **70**, 345 (1948).
- (24) A. Cimino, M. Boudart, and H. S. Taylor, *J. Phys. Chem.*, **58**, 796 (1954).
- (25) D. J. C. Yates, W. F. Taylor, and J. H. Sinfelt, *J. Am. Chem. Soc.*, **86**, 2996 (1964).
- (26) J. H. Sinfelt, *J. Phys. Chem.*, **68**, 344 (1964).
- (27) D. J. C. Yates, J. H. Sinfelt, and W. F. Taylor, *Trans. Faraday Soc.*, **61**, 2044 (1965).
- (28) J. H. Sinfelt, W. F. Taylor, and D. J. C. Yates, *J. Phys. Chem.*, **69**, 95 (1965).
- (29) J. H. Sinfelt and D. J. C. Yates, *J. Catal.*, **8**, 82, 348 (1967); **10**, 362 (1968).
- (30) J. H. Sinfelt and W. F. Taylor, *Trans. Faraday Soc.*, **64**, 3086 (1968).
- (31) J. H. Sinfelt, *J. Catal.*, **27**, 468 (1972).
- (32) R. Coekelbergs, Y. Delannois, A. Frennet, and G. Lienard, *J. Chim. Phys. Phys.-Chim. Biol.*, **61**, 1167 (1964).
- (33) A. Frennet and G. Lienard, *J. Chim. Phys. Phys.-Chim. Biol.*, **68**, 1526 (1971).
- (34) W. P. Neumann, "Plenary Lectures presented at the 4th International Conference on Organometallic Chemistry", Butterworths, London, Bristol, 1969, p 433.
- (35) D. B. Chambers, G. E. Coates, and F. Gloocking, *Discuss. Faraday Soc.*, No. **47**, 157 (1969).
- (36) J. M. Muller and F. G. Gault, *J. Catal.*, **24**, 385 (1972).
- (37) G. Maire, G. Ploudy, J. C. Prudhomme, and F. G. Gault, *J. Catal.*, **4**, 566 (1965).
- (38) D. M. Adams, J. Chatt, R. G. Guy, and N. Sheppard, *J. Chem. Soc.*, 738 (1961).
- (39) F. Garin and F. G. Gault, results to be published.
- (40) J. M. Andre, M. C. Andre, and G. Leroy, *Bull. Soc. Chim. Belg.*, **80**, 265 (1971).